Molecular Crystals and Liquid Crystals

ISSN: 1542-1406 (Print) 1563-5287 (Online) Journal homepage: http://www.tandfonline.com/loi/gmcl20

Crystal Structure Analysis of Betti Base 1-((2-hydroxynaphthalen-1-yl)(2-hydroxyphenyl)methyl)urea•2DMF Solvate

Gudipati Srinivasa Rao, Srinivas Basavoju & Ramachandraiah A

To cite this article: Gudipati Srinivasa Rao, Srinivas Basavoju & Ramachandraiah A (2014) Crystal Structure Analysis of Betti Base 1-((2-hydroxynaphthalen-1-yl)(2-hydroxyphenyl)methyl)urea•2DMF Solvate, Molecular Crystals and Liquid Crystals, 605:1, 225-239, DOI: 10.1080/15421406.2014.905033

To link to this article: http://dx.doi.org/10.1080/15421406.2014.905033

Mol. Cryst. Liq. Cryst., Vol. 605: pp. 225–239, 2014

ISSN: 1542-1406 print/1563-5287 online
DOI: 10.1080/15421406.2014.905033

Crystal Structure Analysis of Betti Base 1-((2-hydroxynaphthalen-1-yl)(2-hydroxyphenyl)methyl)urea●2DMF Solvate

GUDIPATI SRINIVASA RAO, SRINIVAS BASAVOJU, AND RAMACHANDRAIAH A*

Department of Chemistry, National Institute of Technology, Warangal, Telangana, India

A novel Betti base compound, 1-((2-hydroxynaphthalen-1-yl)(2-hydroxyphenyl) methyl)urea, UBB, was synthesized and characterized by spectral, structural and thermal studies. Single crystal X-ray diffraction studies reveal that the racemic mixture of the compound, when crystallized from DMF, yields R-isomer preferentially (prismatic crystals), whereas, when crystallized from 5:1 (v/v) mixture of DMF-THF, it yields S-isomer (rectangular shaped crystals) with two molecules of DMF, included in both the cases. The crystal structure is discussed in terms of supramolecular interactions and molecular modeling. Both R and S enantiomeric DMF solvate crystals are in their chiral triclinic P1 *space group.*

Keywords 1-((2-hydroxynaphthalen-1-yl)(2-hydroxyphenyl)methyl)urea; betti base; molecular modeling; non-centrosymmetric (chiral) space group; supramolecular interactions; thermal analysis.

Introduction

Crystal engineering is a significant subject in identifying new molecular entities in the field of the materials science and pharmaceutical applications [1]. Supramolecular interactions render the synthons some useful credentials such as nonlinear optics (second harmonic generation, SHG activity), ferroelectric, and piezoelectric activity [2, 3], etc. among others. Experimental controls on crystallization frequently result in unusual packing arrangements as desired in rational drug design paradigms involving organic and inorganic hybrid materials [3–7]. One of the ways of obtaining materials with nonlinear optical properties is by crystal engineering of compounds with chiral centers into crystals of noncentrosymmetric (chiral) space groups [8, 9].

Though most of the synthesized amino-naphthols (Betti bases) with asymmetric center crystallize, usually, in the centrosymmetric space groups, occasionally, some of them may

*Address correspondence to Ramachandraiah A, Department of Chemistry, National Institute of Technology, Warangal 506 004, Telangana, India. Tel.: 09490098910.; E-mail: chandraiah@msn.com

Color versions of one or more of the figures in the article can be found online at www.tandfonline.com/gmcl.

crystallize in the noncentrosymmetric space groups [10]. There are several reports on the synthesis of Betti bases by multi-component reactions (MCRs) [11–20]. Here, we report the MCR synthesis of a Betti base using β-naphthol, salicylaldehyde, and urea. The racemic mixture of this Betti base, 1-((2-hydroxynaphthalen-1-yl)(2-hydroxyphenyl)methyl)urea (henceforth, UBB), **1**, is found to be solvent-guided (crystal-engineered) to preferentially crystallize either in R or in S molecular crystals in noncentrosymmetric space groups as revealed by single crystal X-ray diffraction studies.

Experimental

Synthesis

Preparation of 1-((2-hydroxynaphthalen-1-yl)(2-hydroxyphenyl)methyl)urea. The urea Betti base was synthesized by admixing 10 mmol each of salicylaldehyde, 2-naphthol and urea in ethanol under reflux for 10 hr at 80°C (Scheme 1). The crude pale yellow solid obtained, was recrystallized from ethanol. Its solution was found to be racemic.

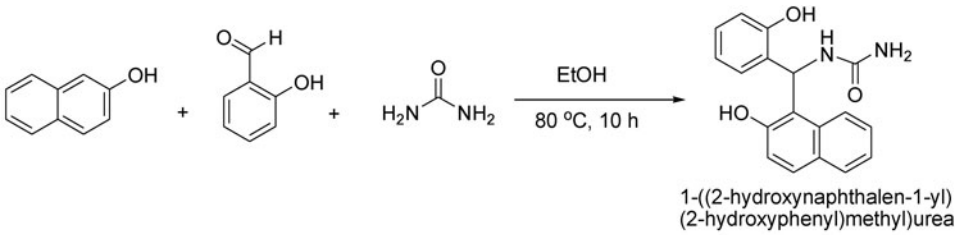

(1)

Scheme 1. Synthesis of 1-((2-hydroxynaphthalen-1-yl)(2-hydroxyphenyl)methyl)urea.

^{1}H NMR (500 MHz, $CDCl_3$): δ 10.38 (s, 1H), 10. 08 (s, H), 7.86 (d, $J = 15$ Hz, 2H), 7.78–7.61(multiplet, 3H), 7.45–7.11(multiplet, 4H), 7.09–6.91 (multiplet, 2H), 6.84 (d, $J = 9$ Hz, 1H), 6.62 (triplet, $J = 10$ Hz, 1H), and 5.82 (s, 1H).

IR: (KBr, Stretching ν_{max}, cm^{-1}): 3457.96 (OH_{sal}), 3373.18 (OH_{naphth}), 3237.01 (NH_2), 1643.33 (C═O), and 1239.29 (C─N).

Crystallization to (R)-UBB.2DMF Solvate. The racemic mixture of UBB (25 mg) was dissolved in hot dimethylformamide (DMF, UV-spectroscopic grade) in a conical flask. The solution was allowed to slow evaporation at ambient temperature for 5 days to obtain light yellow and transparent prismatic shaped crystals.

IR: (KBr, Stretching ν_{max}, cm^{-1}): 3503.90 (OH_{sal}), 3359.18 (OH_{naphth}), 3150.77 (NH_2), 1665.70 (C═O), and 1255.20 (C─N).

Crystallization to (S)-UBB.2DMF Solvate. The racemic mixture of UBB (25 mg) was dissolved in a 5:1 DMF (UV-spectroscopic grade) and tetrahydrofuran (THF, LR grade) under warm conditions. The solution was allowed to slow evaporation at ambient temperature for 4 days to obtain colorless and transparent rectangular-shaped crystals.

IR: (KBr, Stretching ν_{max}, cm^{-1}): 3503.88 (OH_{sal}), 3359.29 (OH_{naphth}), 3151.66 (NH_2), 1665.76 (C═O), and 1255.70 (CN).

Measurements

^{1}H NMR spectra were recorded on a Bruker 500MHz NMR Spectrometer in $CDCl_3$ solution with TMS as the internal standard. A Perkin-Elmer 100S FTIR spectrophotometer was used in the KBr disc for collecting the IR spectra. Differential scanning calorimetric (DSC) thermograms were obtained on a TA Q10 Differential Scanning Calorimeter and data analysis were carried out by the instrument-dedicated TA 2000 software (ver.4.2E). The crystals (∼3 mg) were placed in aluminum crucibles (30 μL) and were scanned at 10 °C/min in the range 30–200 °C under a dry nitrogen atmosphere (flow rate 50 mL/min).

Single Crystal X-ray Diffraction Studies

The shapes of crystals were observed under the LEICA DFC295 polarizing microscope for picking suitable single crystals. The single-crystal X-ray diffraction data of the UBB.2DMF solvate crystals were collected on a Bruker Kappa APEX-II CCD DUO X-Ray Diffractometer at 23°C using graphite-monochromated Mo K_α radiation ($\lambda = 0.71073$ Å). No absorption correction was applied. The lattice parameters were determined from least-squares analysis and the reflection data were integrated using the SHELXTL program [21]. The crystal structures were solved by direct methods using SHELXS-97 and refined by full-matrix least-squares refinement on F^2 with anisotropic displacement parameters for non-H atoms using SHELXL-97 [22]. The phenolic O—H and N—H hydrogen atoms were located from difference Fourier maps. Naphthol O—H, aromatic, and aliphatic C—H hydrogen atoms were generated by the riding model in idealized geometries. The software used to prepare material for publication was Mercury 2.3 (Build RC4), ORTEP-3, and X-Seed [23].

Results and Discussion

Crystal Structure Analysis

The compound (R)-UBB.2DMF crystallizes in the non-centrosymmetric (chiral) triclinic *P*1 space group with one molecule of UBB and two molecules of DMF in the asymmetric unit (Fig. 1a). The UBB molecules in this crystal lattice are exclusively in their R-stereoisomeric absolute configuration. The crystal structure analysis reveals that the UBB and DMF molecules form a one-dimensional triple banded tape-like pattern along the crystallographic *a*-axis with UBB as the central band and the two DMF molecules forming the lateral bands. The naphthol rings are near-parallel to the crystallographic *ab*-planes. The OH group of the phenol is almost coplanar with the benzene ring (torsion angle of H3—O3—C13—C12 is 178.89°) which, in turn, almost, holds the crystallographic *b*-axis. One of the two molecules of DMF, through its C═O oxygen, interacts with NH—CO—NH hydrogen of the urea moiety to form bifurcated C═O···H—N(CO)NH- kind (UBB···DMF) hydrogen bond. The second DMF molecule, through its C═O oxygen, interacts with the phenolic O—H to form C═O···H—O kind (UBB···DMF) hydrogen bond. The β-naphthol O—H group of the UBB interacts with the C═O oxygen of urea moiety of the next UBB molecule to form the 1D tape along the *a*-axis through O—H···O═C (UBB···UBB) hydrogen bond (Fig. 2). The translation related 1D-tapes propagate along the crystallographic *c*-axis via weak C—H···π interactions.

The compound (S)-UBB.2DMF crystallizes in the noncentrosymmetric (chiral) triclinic *P*1 space group with one molecule of UBB and two molecules of DMF in the

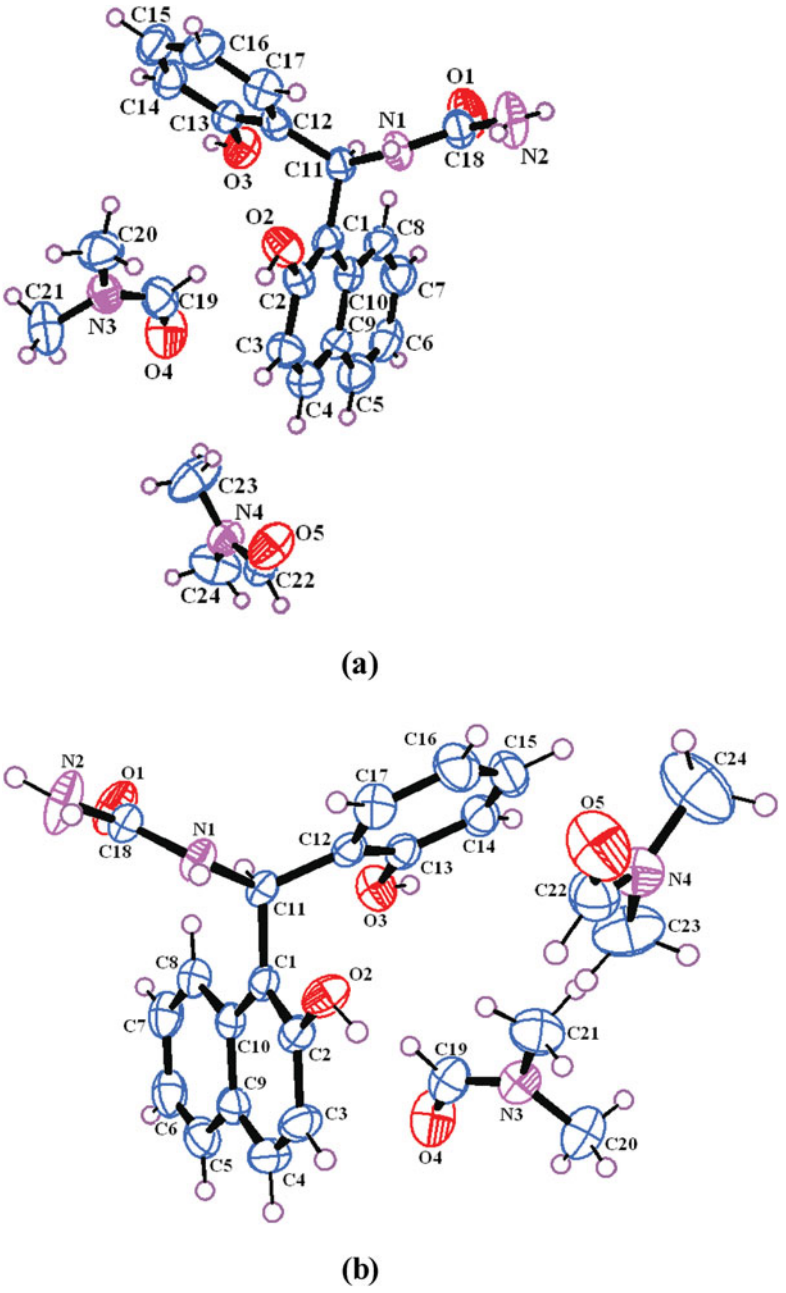

Figure 1. ORTEP representations of Urea Betti base DMF solvates; (a) (R)-UBB.2DMF and (b) (S)-UBB.2DMF. Thermal ellipsoids are drawn at 50% probability level.

asymmetric unit (Fig. 1b). The UBB molecules in this crystal are exclusively in their S-enantiomeric absolute configuration. The crystal structure analysis reveals that the (S)-UBB.2DMF also forms the similar interactions as in (R)-UBB.2DMF with the C═O···H−N(CO)NH-kind hydrogen bonds running along the crystallographic *a*-axis. The

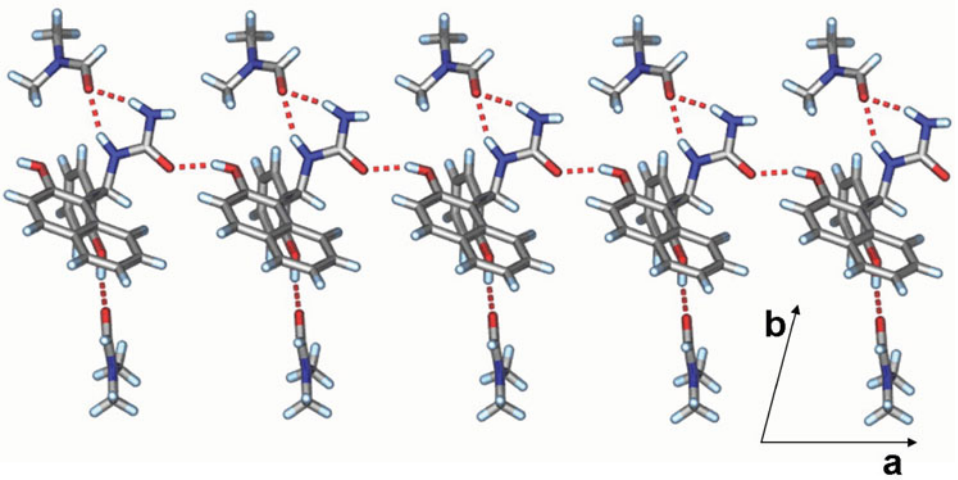

Figure 2. Supramolecular packing in (R)-UBB.2DMF forming one-dimensional triple banded tape-like pattern. Similar interactions can be seen in (S)-UBB.2DMF.

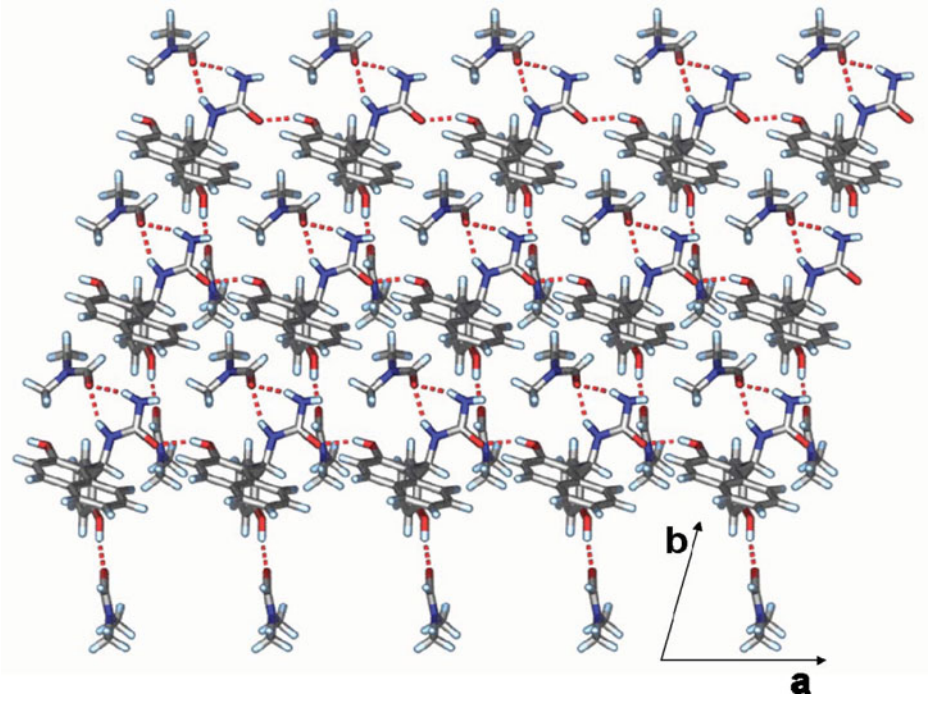

Figure 3. Supramolecular inter-laminar packing in (R)-UBB.2DMF crystal lattice. Similar packing pattern can be seen in (S)-UBB.2DMF.

geometrical parameters of hydrogen bonds are given in Table 2. The Molecular packing array of (R)-UBB.2DMF solvate is shown in Fig. 3 and similar kind of pattern observed in case of (S)-UBB.2DMF solvate. Hence, the two crystal structures (R)-UBB.2DMF and (S)-UBB.2DMF are isostructural (Table 1).

Table 1. Salient crystallographic data and structure refinement parameters of (R)-UBB.2DMF and (S)-UBB.2DMF

	(R)-UBB•2DMF	(S)-UBB•2DMF
Empirical formula	$C_{18}H_{16}N_2O_3$ $2(C_3H_7NO)$	$C_{18}H_{16}N_2O_3$ $2(C_3H_7NO)$
Formula weight	454.52	454.52
Crystal system	Triclinic	Triclinic
Space group	*P*1	*P*1
T/K	296(2)	296(2)
a/Å	7.830(4)	7.8277(11)
b/Å	8.992(5)	8.9915(12)
c/Å	9.388(5)	9.3905(13)
α/°	81.861(9)	81.853(3)
β/°	66.373(9)	66.399(3)
γ/ °	76.413(9)	76.341(4)
Z	1	1
V/Å^3	587.8(5)	587.69(14)
D_{calc}/ g/cm^3	1.284	1.284
F(000)	242.0	242.0
μ/mm^{-1}	0.091	0.091
θ/°	2.33 to 28.00	2.33 to 28.00
Index ranges	$-10 \le h \le 10$ $-11 \le k \le 11$ $-12 \le l \le 12$	$-10 \le h \le 10$ $-10 \le k \le 11$ $-12 \le l \le 12$
N-total	7489	10659
N-independent	4607	4847
N-observed	1905	4420
Parameters	318	312
R_1 ($I > 2\sigma(I)$)	0.0587	0.0339
wR_2 (all data)	0.1007	0.0843
GOF	0.954	1.028
CCDC	945791	—

Differential Scanning Calorimetry. The stereochemical vividity of UBB in racemic mixture, (R)-UBB.2DMF and (S)-UBB.2DMF and certain degree of anisomorphism between (R)-UBB.2DMF and (S)-UBB.2DMF crystals is further reflected in their DSC studies. The DSC thermograms of UBB racemic mixture and the DMF solvates of both the enantiomers are shown in Fig. 4. The DSC trace of racemic UBB shows an endotherm at 183°C corresponding to its melting event. No thermal events are found below this temperature. This fact indicates that no solvent molecules intruded into the polycrystalline racemic mixture during the preparation or recrystallization from ethanol. The crystals obtained from DMF (prismatic shaped crystals), i.e., of (R)-UBB.2DMF, however, exhibit two endotherms at ∼137 and ∼155°C. The event at ∼137°C is assigned to the expulsion of DMF molecules from the solvate crystals whereas that at ∼155°C is to the melting process of the desolvated R enantiomeric crystal residue. The lower melting point of the solvate when compared to the melting point of unsolvated racemic mixture is attributed to (i) strained molecular

Table 2. Geometrical parameters of hydrogen bonds in (R)-UBB.2DMF and (S)-UBB.2DMF

	D···A (Å) UBB.2DMF		H···A (Å) UBB.2DMF		D−H···A (°) UBB.2DMF		Symmetry code UBB.2DMF	
D−H···A[a]	R	S	R	S	R	S	R	S
N(1)−H(1)···O(4)	2.906(6)	2.930(2)	1.99	2.04	150	146	x,1+y,z	x,−1+y,z
O(2)−H(2)···O(1)	2.649(6)	2.664(2)	1.75	1.69	151	172	−1+x,y, z	1+x,y,z
N(2)−H(2B)···O(4)	2.842(10)	2.853(3)	1.88	1.94	159	149	x,1+y,z	x,−1+y,z
O(3)−H(3A)···O(5)	2.738(5)	2.729(2)	1.78	1.75	165	171	1+x,y,−1+z	−1+x,1+y,z
C(4)−H(4)···O(5)	3.671(7)	3.669(2)	2.62	2.62	163	164	—	x,1+y,−1+z
Intra C(8)−H(8)···O(1)	3.579(7)	3.553(2)	2.77	2.73	132	132	—	—
C(19)−H(19)···O(3)	3.491(8)	3.499(3)	2.66	2.68	133	132	—	—
C(20)−H(20C)···O(1)	3.760(7)	—	2.75	—	156	—	−1+x,y,z	—
C(21)−H(21A)···O(2)	3.801(7)	3.923(3)	2.79	2.94	156	151	x,−1+y,z	—
C(21)−H(21C)···O(3)	3.603(9)	—	2.67	—	143	—	−1+x,y,z	—
C(24)−H(24A)···O(1)	3.746(8)	—	2.67	—	175	—	−1+x,−1+y,1+z	—
C(14)−H(14)···O(5)	3.405(7)	3.397(2)	2.65	2.65	126	126	1+x,y,−1+z	−1+x,1+y,z
C(20)−H(20A)···O(2)	—	3.805(3)	—	2.8	—	155	—	x,1+y,z
C(20)−H(20B)···O(3)	—	3.591(3)	—	2.65	—	145	—	1+x,y,z
C(23)−H(23C)···O(1)	—	3.749(3)	—	2.67	—	172	—	1+x,y,z

orientations of UBB in solvates (vis a vis the racemic compound) and (ii) the depression in freezing point by colligative property.

The thermogram of (S)-UBB.2DMF (rectangular shaped crystals) shows two endotherms at ∼144 and ∼155°C. The event at ∼144°C is again assigned to the expulsion of DMF molecules from the solvate crystals whereas that at ∼155°C is, as usual, to the melting process of the desolvated S enantiomeric crystal residue. That the desolvation point of (R)-UBB.2DMF is lower than that of (S)-UBB.2DMF by ∼7 C° is unexpected. One can relate this anomaly to possible anisotropic packing of UBB···UBB

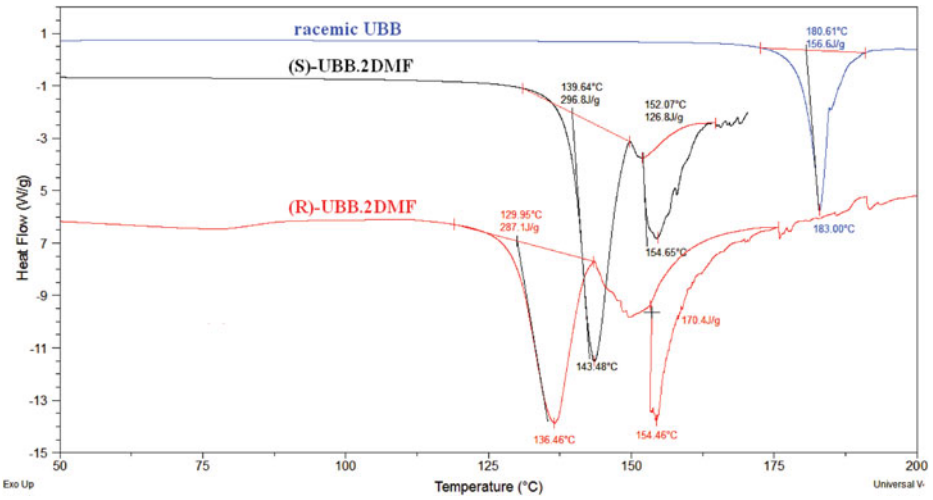

Figure 4. DSC thermograms of racemic UBB, (R)-UBB.2DMF and (S)-UBB.2DMF.

and UBB···DMF by supramolecular (intermolecular) interactions. Some of the other crystallographic and molecular data shown in Table 3 for (R)-UBB.2DMF and (S)-UBB.2DMF also comply with higher desolvation temperature for (S)-UBB.2DMF than (R)-UBB.2DMF. The heat of desolvation is found to be more for (S)-UBB.2DMF (+134.80 kJ mol^{-1}) solvate than that for (R)-UBB.2DMF (+130.4 kJ mol^{-1}) solvate. Hence, the binding energy of DMF molecules in (S)-UBB.2DMF is evaluated as −67.4 kJ mol^{-1} whereas that in (R)-UBB.2DMF as −65.2 kJ mol^{-1}, implying that the DMF molecules are held more firmly in (S)-UBB.2DMF than in (R)-UBB.2DMF.

CSD Analysis. A CSD (ConQuest version 5.34, Nov 2012, number of hits 624 927) search for Betti bases was performed. A typical Betti base structure was drawn and search was performed. A total of 114 Betti base crystal structures were found. Among them six structures do not possess 3D coordinates (refcodes: ALOXAA, FOZZEA, KEFZEB01, PEVNEK01, WIXCEM01, and WIXTED01) and 5 are metal complexes (refcodes: RARVOX, QOMNAI, QOMNOW, QOMPAK, and SAPWUC); and 12 are solvates (refcodes: GEFGAB, BADQUS, CUYMUE, JETJEY, LAQLAS, NUBZOA, NUBZUG, QOMNAI, SAPWUC, UPUBAJ, WIXTED, and XAYBEF).

Infrared Spectral Studies and Molecular Modeling of free Molecule. The differences between the stretching frequencies of the bonds of the solvate enantiomers with reference to the racemic compound are shown in Fig. 6. It is clear that the stretching frequencies of the $(O{-}H)_{sal}$, C−O, and C(11)−N(1) of racemic solid UBB are lower than those of R and S DMF solvates. This suggests that these three bonds acquire greater strength upon solvation. However, the stretching frequency of $(O{-}H)_{naphth}$ and $(N(2){-}H)_{urea}$ are higher for the racemic compound than those of R and S DMF solvates indicating lowering of

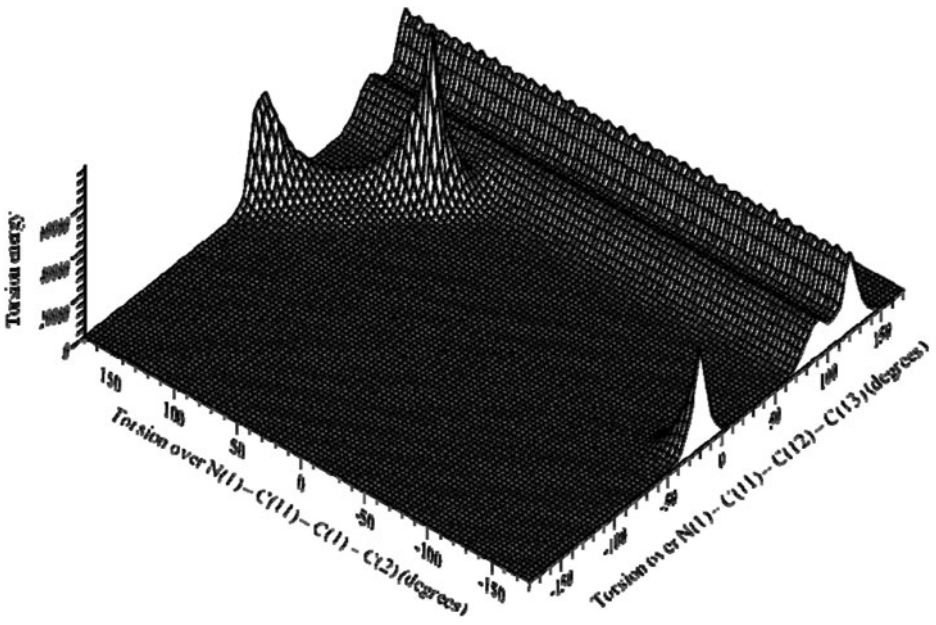

Figure 5. Double dihedral torsional energy plot over N(1)−C(11)−C(1)−C(2) and N(1)−C(11)−C(12)−C(13) planes.

Table 3. Bond lengths (Å), bond angles (°) for (R)-UBB.2DMF, (S)-UBB.2DMF from XRD data and nonsolvated UBB from molecular modeling

Atoms	(R) – UBB.2DMF XRD data (q1)	(S) – UBB.2DMF XRD data (q2)	Nonsolvated UBB Molecular modeling Molecular modeling data (q3)
C(14)–C(15)	1.372(7)	1.370(3)	1.4205
C(14)–C(13)	1.374(6)	1.394(2)	1.4265
C(14)–H(14)	0.93	0.93	1.1024
C(17)–C(12)	1.378(6)	1.383(2)	1.4288
C(17)–C(16)	1.386(7)	1.389(3)	1.422
C(17)–H(17)	0.93	0.93	1.1004
N(1)–C(18)	1.337(6)	1.3392(19)	1.3697
N(1)–C(11)	1.469(5)	1.4571(19)	1.4662
N(1)–H(1)	0.97(10)	0.79(2)	1.0183
O(1)–C(18)	1.253(6)	1.230(2)	1.2044
N(2)–C(18)	1.344(7)	1.345(2)	1.3611
N(2)–H(2A)	0.81(6)	0.86	1.0102
N(2)–H(2B)	0.88(5)	0.86	1.0103
C(3)–C(4)	1.347(7)	1.348(3)	1.4186
C(3)–C(2)	1.411(6)	1.417(2)	1.4237
C(3)–H(3)	0.93	0.93	0.9689
O(2)–C(2)	1.376(5)	1.3574(19)	1.3588
O(2)–H(2)	0.82	0.82	0.9704
O(5)–C(22)	1.232(6)	1.222(2)	—
C(24)–N(4)	1.458(6)	1.438(3)	—
C(24)–H(24A)	0.96	0.96	—
C(24)–H(24B)	0.96	0.96	—
C(24)–H(24C)	0.96	0.96	—
O(4)–C(19)	1.237(6)	1.225(2)	—
C(11)–C(12)	1.532(6)	1.5286(19)	1.5207
C(11)–C(1)	1.533(6)	1.5266(19)	1.5193
C(11)–H(11)	0.98	0.98	1.117
C(1)–C(2)	1.370(6)	1.3836(19)	1.4327
C(1)–C(10)	1.421(6)	1.430(2)	1.4369
C(10)–C(8)	1.415(6)	1.421(2)	1.4308
C(10)–C(9)	1.423(6)	1.428(2)	1.4298
C(9)–C(5)	1.405(7)	1.413(3)	1.4266
C(9)–C(4)	1.406(7)	1.413(3)	1.4225
N(4)–C(22)	1.306(6)	1.318(2)	—
N(4)–C(23)	1.434(7)	1.455(3)	—
N(3)–C(19)	1.305(6)	1.321(2)	—
N(3)–C(21)	1.447(6)	1.455(3)	—
N(3)–C(20)	1.459(6)	1.452(3)	—
C(15)–C(16)	1.376(7)	1.375(3)	1.4196
C(15)–H(15)	0.93	0.93	1.1015
C(5)–C(6)	1.357(8)	1.357(3)	1.4212

(Continued on next page)

Table 3. Bond lengths (Å), bond angles (°) for (R)-UBB.2DMF, (S)-UBB.2DMF from XRD data and nonsolvated UBB from molecular modeling *(Continued)*

Atoms	(R) – UBB.2DMF XRD data (q1)	(S) –UBB.2DMF XRD data (q2)	Nonsolvated UBB Molecular modeling Molecular modeling data (q3)
C(5)–H(5)	0.93	0.93	1.1021
C(6)–C(7)	1.388(8)	1.401(3)	1.4207
C(6)–H(6)	0.93	0.93	1.1016
C(16)–H(16)	0.93	0.93	1.1017
C(4)–H(4)	0.93	0.93	1.1018
C(8)–C(7)	1.363(7)	1.364(2)	1.4231
C(8)–H(8)	0.93	0.93	1.1001
C(7)–H(7)	0.93	0.93	1.102
C(22)–H(22)	0.93	0.93	—
C(23)–H(23A)	0.96	0.96	—
C(23)–H(23B)	0.96	0.96	—
C(23)–H(23C)	0.96	0.96	—
C(19)–H(19)	0.93	0.93	—
C(21)–H(21A)	0.96	0.96	—
C(21)–H(21B)	0.96	0.96	—
C(21)–H(21C)	0.96	0.96	—
C(20)–H(20A)	0.96	0.96	—
C(20)–H(20B)	0.96	0.96	—
C(20)–H(20C)	0.96	0.96	—
C(13)–O(3)	1.378(6)	1.363(2)	1.3599
C(13)–C(12)	1.393(6)	1.396(2)	1.4343
O(3)–H(3A)	0.96(5)	0.92(3)	0.9689
C(15)–C(14)–C(13)	120.7(5)	120.35(17)	121.975
C(15)–C(14)–H(14)	119.7	119.8	118.949
C(13)–C(14)–H(14)	119.7	119.8	119.076
C(12)–C(17)–C(16)	121.6(5)	121.17(17)	121.976
C(12)–C(17)–H(17)	119.2	119.4	121.213
C(16)–C(17)–H(17)	119.2	119.4	116.805
C(18)–N(1)–C(11)	121.2(4)	122.06(14)	122.86
C(18)–N(1)–H(1)	116(6)	116.4(14)	118.824
C(11)–N(1)–H(1)	123(6)	120.5(14)	118.273
C(18)–N(2)–H(2A)	103(4)	120	117.451
C(18)–N(2)–H(2B)	112(3)	120	121.198
H(2A)–N(2)–H(2B)	144(5)	120	121.351
C(4)–C(3)–C(2)	119.8(5)	120.44(15)	121.456
C(4)–C(3)–H(3)	120.1	119.8	119.254
C(2)–C(3)–H(3)	120.1	119.8	119.286
C(2)–O(2)–H(2)	109.5	109.5	110.177
N(4)–C(24)–H(24A)	109.5	109.5	—
N(4)–C(24)–H(24B)	109.5	109.5	—
H(24A)–C(24)–H(24B)	109.5	109.5	—

(Continued on next page)

Table 3. Bond lengths (Å), bond angles (°) for (R)-UBB.2DMF, (S)-UBB.2DMF from XRD data and nonsolvated UBB from molecular modeling *(Continued)*

Atoms	(R) – UBB.2DMF XRD data (q1)	(S) –UBB.2DMF XRD data (q2)	Nonsolvated UBB Molecular modeling Molecular modeling data (q3)
H(24A)–C(24)–H(24C)	109.5	109.5	—
H(24B)–C(24)–H(24C)	109.5	109.5	—
N(1)–C(11)–C(12)	111.8(4)	112.47(12)	113.167
N(1)–C(11)–C(1)	111.0(3)	110.66(11)	108.875
C(12)–C(11)–C(1)	113.6(4)	114.00(10)	118.273
N(1)–C(11)–H(11)	106.7	106.4	106.831
C(12)–C(11)–H(11)	106.6	106.4	100.544
C(1)–C(11)–H(11)	106.6	106.4	108.161
C(2)–C(1)–C(10)	118.4(4)	118.71(12)	119.44
C(2)–C(1)–C(11)	120.2(4)	119.88(13)	120.315
C(10)–C(1)–C(11)	121.3(4)	121.36(12)	120.223
C(8)–C(10)–C(1)	123.7(5)	123.35(13)	122.321
C(8)–C(10)–C(9)	116.2(4)	117.27(14)	117.305
C(1)–C(10)–C(9)	120.1(5)	119.37(14)	120.367
C(5)–C(9)–C(4)	121.3(6)	121.83(15)	119.067
C(5)–C(9)–C(10)	120.6(5)	119.07(16)	121.132
C(4)–C(9)–C(10)	118.1(5)	119.10(15)	119.8
O(1)–C(18)–N(1)	122.3(5)	122.30(15)	122.324
O(1)–C(18)–N(2)	121.3(6)	121.94(14)	119.283
N(1)–C(18)–N(2)	116.2(6)	115.74(16)	118.392
C(1)–C(2)–O(2)	118.7(4)	118.36(12)	121.995
C(1)–C(2)–C(3)	121.6(5)	121.18(14)	119.216
O(2)–C(2)–C(3)	119.7(5)	120.43(13)	118.777
C(22)–N(4)–C(23)	120.7(5)	121.22(18)	—
C(22)–N(4)–C(24)	122.5(5)	121.08(17)	—
C(23)–N(4)–C(24)	116.8(5)	117.69(19)	—
C(19)–N(3)–C(21)	120.3(5)	121.53(17)	—
C(19)–N(3)–C(20)	121.9(5)	120.16(17)	—
C(21)–N(3)–C(20)	117.8(5)	118.30(17)	—
C(14)–C(15)–C(16)	119.2(5)	119.78(16)	118.954
C(14)–C(15)–H(15)	120.4	120.1	120.533
C(16)–C(15)–H(15)	120.4	120.1	120.511
C(6)–C(5)–C(9)	120.6(6)	122.08(17)	120.54
C(6)–C(5)–H(5)	119.7	119	118.866
C(9)–C(5)–H(5)	119.7	119	120.594
C(5)–C(6)–C(7)	119.9(5)	119.02(17)	119.1
C(5)–C(6)–H(6)	120.1	120.5	120.475
C(7)–C(6)–H(6)	120.1	120.5	120.412
C(15)–C(16)–C(17)	120.0(5)	120.18(18)	119.534
C(15)–C(16)–H(16)	120	119.9	120.091

(Continued on next page)

Table 3. Bond lengths (Å), bond angles (°) for (R)-UBB.2DMF, (S)-UBB.2DMF from XRD data and nonsolvated UBB from molecular modeling *(Continued)*

Atoms	(R) – UBB.2DMF XRD data (q1)	(S) –UBB.2DMF XRD data (q2)	Nonsolvated UBB Molecular modeling Molecular modeling data (q3)
C(17)–C(16)–H(16)	120	119.9	120.372
C(3)–C(4)–C(9)	121.8(5)	121.10(14)	119.617
C(3)–C(4)–H(4)	119.1	119.5	119.353
C(9)–C(4)–H(4)	119.1	119.5	121.022
C(7)–C(8)–C(10)	121.8(5)	121.38(15)	121.755
C(7)–C(8)–H(8)	119.1	119.3	116.331
C(10)–C(8)–H(8)	119.1	119.3	121.91
C(8)–C(7)–C(6)	120.9(6)	121.17(18)	120.07
C(8)–C(7)–H(7)	119.6	119.4	120.136
C(6)–C(7)–H(7)	119.6	119.4	119.792
O(5)–C(22)–N(4)	125.2(5)	125.32(17)	—
O(5)–C(22)–H(22)	117.4	117.3	—
N(4)–C(22)–H(22)	117.4	117.3	—
N(4)–C(23)–H(23A)	109.5	109.5	—
N(4)–C(23)–H(23B)	109.5	109.5	—
H(23A)–C(23)–H(23B)	109.5	109.5	—
N(4)–C(23)–H(23C)	109.5	109.5	—
H(23A)–C(23)–H(23C)	109.5	109.5	—
H(23B)–C(23)–H(23C)	109.5	109.5	—
O(4)–C(19)–N(3)	125.4(5)	125.18(18)	—
O(4)–C(19)–H(19)	117.3	117.4	—
N(3)–C(19)–H(19)	117.3	117.4	—
N(3)–C(21)–H(21A)	109.5	109.5	—
N(3)–C(21)–H(21B)	109.5	109.5	—
H(21A)–C(21)–H(21B)	109.5	109.5	—
N(3)–C(21)–H(21C)	109.5	109.5	—
H(21A)–C(21)–H(21C)	109.5	109.5	—
H(21B)–C(21)–H(21C)	109.5	109.5	—
N(3)–C(20)–H(20A)	109.5	109.5	—
N(3)–C(20)–H(20B)	109.5	109.5	—
H(20A)–C(20)–H(20B)	109.5	109.5	—
N(3)–C(20)–H(20C)	109.5	109.5	—
H(20A)–C(20)–H(20C)	109.5	109.5	—
H(20B)–C(20)–H(20C)	109.5	109.5	—
C(14)–C(13)–O(3)	122.3(4)	121.99(15)	118.871
C(14)–C(13)–C(12)	121.1(5)	120.51(15)	119.17
O(3)–C(13)–C(12)	116.6(4)	117.49(13)	121.864
C(17)–C(12)–C(13)	117.4(4)	117.99(13)	118.316
C(17)–C(12)–C(11)	123.6(4)	123.56(14)	120.906
C(13)–C(12)–C(11)	118.9(4)	118.36(13)	120.672
C(13)–O(3)–H(3A)	117(3)	114.9(18)	110.004

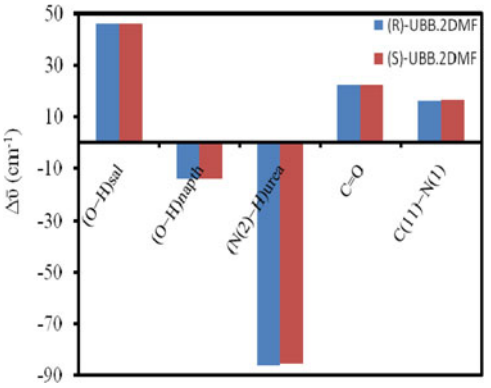

Figure 6. Histographic presentation of FTIR data of stretching frequency of some selected bonds of the solids.

these bond strengths upon solvation. The $(O{-}H)_{naphth}$ is not suitably positioned in the free molecule for any intramolecular hydrogen bonding, whereas, it is engaged in solvation through hydrogen bond with the DMF solvent molecules. Same is true with NH_2 moiety. It is well-known fact, that the bond strength and hence the stretching frequency of X−H bond decreases upon hydrogen bonding as X−H···*Y*, where *Y* is the donor atom (electronegative). On this basis one can account why the stretching frequency of NH_2 and $(O{-}H)_{naphth}$ decrease upon solvation with DMF molecule through hydrogen bonding. It is also a fact that intramolecular hydrogen bond usually is stronger than intermolecular hydrogen bond. The $(O{-}H)_{sal}$, C=O, and C(11)−N(1) bonds are engaged in intramolecular hydrogen bonding in free molecule as evident from molecular modeling. However, these bonds have to detach themselves from intramolecular hydrogen bond in order to solvate with DMF molecules via intermolecular hydrogen bond. This is the reason why, perhaps the stretching frequency of these free moieties increase upon solvation. Molecular modeling studies were carried out on nonsolvated UBB using ChemOffice Ultra (Version 11.0) to obtain the molecular geometric properties and other relevant structural data. In Table 2 are placed some of the intramolecular and intermolecular hydrogen bond lengths and bond

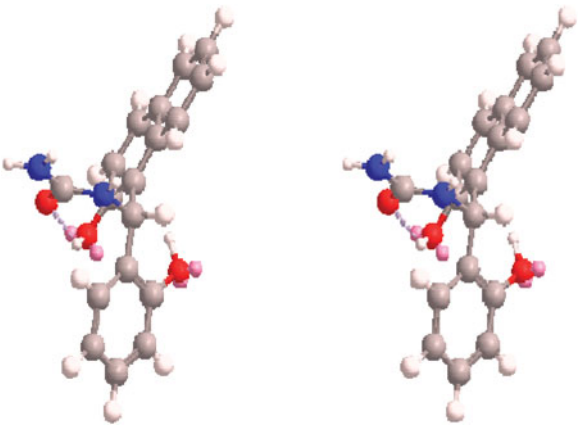

Figure 7. Stereographic image of the energy-minimized structure of UBB gas phase molecule.

angles whereas in Table 3, some of the most relevant bond lengths and bond angles gained from X-ray crystallography along with those from molecular modeling are tabulated. The respective experimental and modeled data are in good agreement for many of the bonds and bond angles, whereas, torsional energy conformational Double dihedral 3D plot is shown in Fig. 5. It is observed that the bond lengths and bond angles are slightly varied from the experimental X-ray data and that of simulated data points involving atoms interacting with DMF molecules of the solvates. The structure of the energy minimized free molecule is shown in Fig. 7 in its stereographic vision.

Conclusions

A Betti base, 1-((2-hydroxynaphthalen-1-yl)(2-hydroxyphenyl)methyl)urea, UBB, was prepared and found to give solvated crystals, as (R)-UBB.2DMF and (S)-UBB.2DMF when UBB was recrystallized from DMF and DMF-THF solvent systems, respectively. The two enantiomeric solvates crystallized in a noncentrosymmetric (chiral) triclinic *P*1 space group with isomorphous and the two crystal structures are isostructural. The betti base and DMF molecules in the crystal structure form supramolecular one-dimensional triple banded tape-like pattern with O—H···O and N—H···O hydrogen bonds.

Acknowledgments

GSR expresses his thanks to the Director, National Institute of Technology Warangal for awarding Institute Fellowship.

References

[1] Desiraju, G. R. (1989) *Crystal Engineering: The Design of Organic Solids*, Elsevier: Amsterdam.
[2] Muthuraman, M., LeFur, Y., Bagieu-Beucher, M., Masse, R., Nicoud, J. F., George, S., Nangia, A., & Desiraju, G. R. (2000). *J. Solid State Chem.*, *152*, 221–228.
[3] Holman, K. T., Pivovar, A. M. & Ward, M. D. (2001). *Science*, *294*, 1907.
[4] Hollingsworth, M. D. (2002). *Science*, *295*, 2410.
[5] Thalladi, V. R., Brasselet, S., Weiss, H. C., Blaser, D., Katz, A. K., Carrell, H. L., Boese, R., Zyss, J., Nangia, A., & Desiraju, G. R. (1998). *J. Am. Chem. Soc.*, *120*, 2563.
[6] Braga, D., Grepioni, F., & Desiraju, G. R. (1998). *Chem. Rev.*, *98*, 1375.
[7] Long, N. J. (1995). *Angew. Chem. Int. Ed.*, *34*, 21.
[8] Yuan, Z., Mengting, H., Qiong, Y., & Rengen, X. (2010). *Chin. J. Chem.*, *28*. 1533.
[9] Zhao, H., Li, Y. H., Wang, X. S., Qu, Z. R., Wang, L. Z., Xiong, R. G., Abrahams, B. F., & Xue, Z. L. (2004). *Chem. Eur. J.*, *10*, 2386–2390.
[10] Yuan, Z., Meng-Ting, H., Qiong, Y., & Gen, X. R. (2010). *Chin. J. Chem.*, *28*(9), 1533–1537.
[11] (a) Cosimo, C., Maria, A. M. C., Angel, A. L., Piniella, J. F., & Francesco, C. (2012). *CrystEngComm.*, *14*, 3972. (b) Wang, W. X. (2012). *Acta Cryst.*, *E68*, o884. (c) Zhao, Q. (2012). *Acta Cryst.*, *E68*, o529. (d) Shu, L. J. (2011). *Acta Cryst.*, *E67*, o1681. (e) Ni, H. M. (2011). *Acta Cryst.*, *E67*, o322. (f) Chen, X. Y., Zhao, M. M., Qian, X., & Hou, S. G. (2011). *Acta Cryst.*, *E67*, o3484. (g) Chen, J. M., & Zhao, H. (2010). *Acta Cryst.*, *E66*, o3118. (h) Xiao, J., & Zhao, H. (2010). *Acta Cryst.*, *E66*, o2938. (i) Xue, M. W. (2010). *Acta Cryst.*, *E66*, o2006. (j) Wang, W. X., & Zhao, H. (2009). *Acta Cryst.*, *E65*, o1277. (k) Zhang, Y., & Li, Y. H. (2009). *Acta Cryst.*, *E65*, o2257. (l) NizamMohideen, M., Thenmozhi, S., SubbiahPandi, A., Panneer Selvamc, N., & Perumalc, P. T. (2009). *Acta Cryst.*, *E65*, o740. (m) NizamMohideen, M., Subbiah Pandi, A., Panneer Selvamc, N., & Perumalc, P. T. (2009). *Acta Cryst.*, *E65*, o714–o715. (n) Wang, W. X., & Zhao, H. (2008). *Acta Cryst.*, *E64*, o1900. (o) Wan, C., & Zhao, H. (2008). *Acta Cryst.*, *E64*, o1926. (p) Li, Y. H., Zhao, M. M., & Zhang, Y. (2008). *Acta Cryst.*, *E64*, o2005. (q) Huang,

X. T., Lin, K., Ji, T., Tang, G., & Zhao, Y. F. (2007). *Acta Cryst.*, *E63*, o3031. (r) Qu, Z. R. (2007). *Acta Cryst.*, *E63*, o3429. (s) Mosslemin, M. H., Arab-Salmanabadi, S., & Masoudi, M. (2007). *Acta Cryst.*, *E63*, o444–o445. (t) Bazgir, A., Amani, V., & Khavasi, H. R. (2006). *Acta Cryst.*, *E62*, o3875–o3876. (u) Bazgir, A., Amani, V., & Khavasi, H. R. (2006). *Acta Cryst.*, *E62*, o3533–o3534. (v) Bazgir, A., Amani, V., & Khavasi, H. R. (2006). *Acta Cryst.*, *E62*, o5523–o5524.

[12] Selvam, N. P., & Perumal, P. T. (2008). *Tetrahedron*, *64*, 2972–2978.

[13] Selvam, N. P., & Perumal, P. T. (2006). *Tetrahedron Letters*, *47*, 7481–7483.

[14] Xu, L., Shen, X., Zhang, C., & Mikami, K. (2005). *Chirality*, *17*, 476–480.

[15] Szatmári, I., Sillanpää, R., & Fülöp, F. (2008). *Tetrahedron: Asymmetry*, *19*, 612–617

[16] Periasamy, M., Narsi Reddy, M., & Anwar, S. (2004). *Tetrahedron: Asymmetry.*, *15*, 1809–1812.

[17] Cardellicchio, C., Ciccarella, G., Naso, F., Schingaro, E., & Scordari, F. (1998). *Tetrahedron: Asymmetry*, *9*, 3667–3675.

[18] Lu, J., Xu, X., Wang, S., Wang, C., Hu, Y., & Hu, H. (2002). *J. Chem. Soc., Perkin Trans.*, *1*, 2900–2903.

[19] Clive, D. L. J., & Ardelean, E. S. (2001). *J. Org. Chem.*, *66*(14), 4841–4844.

[20] Liu, D. X., Zhang, L. C., Wang, Q., Da, C. S., Xin, Z. Q., Wang, R., Choi, M. C. K., & Chan, A. S. C. (2001). *Organic Letters*, *3*(17), 2733–2735.

[21] SHELXTL. Program for the Solution and Refinement of Crystal Structures, (version 6.14); Bruker AXS: Wisconsin, USA, 2000.

[22] Sheldrick, G. M. (1997). *SHELX-97: Program for the Solution and refinement of Crystal Structures*, University of Göttingen: Germany.

[23] (a) Macrae, C. F., Bruno, I. J., Chisholm, J. A., Edgington, P. R., McCabe, P., Pidcock, E., Rodriguez-Monge, L., Taylor, R., van de Streek, J., & Wood, P. A. (2008). *J. Appl. Cryst.*, *41* 466. (b) Burnett, M. N., & Johnson, C. K. (1996) ORTEPIII, Report ORNL-6895, Oak Ridge National Laboratory, Tennessee, USA); Farrugia, L. J. (1997). *J. Appl. Cryst., 30* 565. (c) Barbour, L. J. (2001)"X-Seed-A software tool for supramolecular crystallography" *J. Supramol. Chem.*, *1*, 189.